*American Mineralogist, Volume 71, pages 1494–1501, 1986*

# Crystal structure of the zeolite mineral goosecreekite, $CaAl_2Si_6O_{16} \cdot 5H_2O$*

**Roland C. Rouse, Donald R. Peacor**
Department of Geological Sciences, University of Michigan, Ann Arbor, Michigan 48109, U.S.A.

## Abstract

The zeolite mineral goosecreekite ($CaAl_2Si_6O_{16} \cdot 5H_2O$) is monoclinic, $P2_1$, with $a$ = 7.401(3), $b$ = 17.439(6), $c$ = 7.293(3) Å, $\beta$ = 105.44(4)°, and Z = 2. Its structure has been solved by Fourier and direct methods and refined to an unweighted residual of 0.061 using 2017 reflections. Three sets of intersecting channels parallel to the **a**, **b**, and **c*** axes, respectively, contain Ca atoms coordinated by two framework oxygens and five water molecules arranged in a distorted monocapped octahedron. The framework consists of $SiO_4$ and $AlO_4$ tetrahedra grouped into 4-, 6-, and 8-membered rings, which share edges to form distorted layers parallel to (010). Si-Al ordering is almost complete, with two out of six tetrahedral sites showing minor solid solution. The (010) layers resemble those in brewsterite [$(Sr,Ba)Al_2Si_6O_{16} \cdot 5H_2O$] but are cross-linked in a different way to form the 3-dimensional framework. The structure can also be described in terms of $T_9O_{18}$ units, which form vertex-sharing chains in the **b** direction, adjacent chains being linked in the **a** and **c** directions by 4-rings. Goosecreekite cannot readily be assigned to any of the known zeolite families.

## Introduction

In 1980 Dunn et al. described a new species of zeolite, which they named goosecreekite after the type locality in Loudon County, Virginia. A chemical and crystallographic study yielded the formula $CaAl_2Si_6O_{16} \cdot 5H_2O$ with Z = 2 and a monoclinic cell of symmetry $P2_1$ or $P2_1/m$ with parameters $a$ = 7.52(2), $b$ = 17.56(3), $c$ = 7.35(2) Å, and $\beta$ = 105.71°. Dunn et al. also noted the resemblance between the formula of goosecreekite and those of epistilibite [$(Ca,Na)Al_2Si_6O_{16} \cdot 5H_2O$] and brewsterite [$(Sr,Ba)Al_2Si_6O_{16} \cdot 5H_2O$] and the fact that its unit cell and space group were strikingly similar to those of brewsterite. On this basis they proposed that goosecreekite belongs to the heulandite group, which consists of heulandite, clinoptilolite, brewsterite, stilbite, barrerite, and stellerite (Barrer, 1984), with a structure perhaps related to that of brewsterite. An analysis of the crystal structure of goosecreekite, details of which are reported here, has confirmed the second part of this hypothesis but not the first. Goosecreekite is not a member of the heulandite group and, indeed, does not readily fit into any of the known zeolite families.

## Experimental methods

Most goosecreekite is unsuitable for intensity measurement owing to its pronounced lineage structure, but with some effort a nearly euhedral crystal of dimensions 0.27 × 0.17 × 0.27 mm and exceptional quality was located. From this crystal the intensities of 2017 reflections having $\sin\theta \leq 0.46$ were measured with a Supper-Pace diffractometer system employing Weissenberg equi-inclination geometry, graphite-crystal–monochromatized Mo$K\alpha$ radiation, and a scan rate of 2°/min. The intensities were converted to structure-factor amplitudes by correction for Lorentz, polarization, and absorption effects ($\mu_l$ = 9.23 cm$^{-1}$). Only 79 of the 2017 reflections were unobserved. Structure factor calculations and refinement were carried out with the program RFINE 2 (Finger, 1972) using neutral-atom scattering factors (Doyle and Turner, 1968) and the reciprocal variances of the $|F|_{obs}$ as weights. Anomalous dispersion corrections were very small and were therefore neglected.

The unit-cell parameters of goosecreekite were redetermined by least-squares refinement of powder-diffractometer data, which had been obtained using as an internal standard the high-purity quartz ($a$ = 4.9137, $c$ = 5.4053 Å) studied by Frondel and Hurlbut (1955). The resulting values, $a$ = 7.401(3), $b$ = 17.439(6), $c$ = 7.293(3) Å, and $\beta$ = 105.44(4)°, are more accurate than those obtained by Dunn et al. (1980) using Gandolfi film data, and they were therefore used in the present study. The superiority of the new parameters is evident both from their smaller estimated standard deviations and the fact that they yield better agreement between measured and calculated densities. The measured, newly calculated, and old calculated densities are 2.21, 2.23, and 2.16 g/cm$^3$, respectively.

Attempts to deduce the structure of goosecreekite from that of brewsterite (Perrotta and Smith, 1964; Schlenker et al., 1977; Artioli et al., 1985) and from the Patterson function were fruitless, and so a solution by direct methods was tried using the program MULTAN 78 (Main, 1978). Statistical tests performed by MULTAN indicated unequivocally that the structure is noncentrosymmetric, i.e., the space group is $P2_1$, and a calculation of phase sets yielded one having a combined figure of merit of 3.00. The nine largest peaks in the corresponding E-map proved, upon calculation of structure factors and interatomic distances, to represent the nine nonequivalent cations (Ca + 8 tetrahedral cations) in the goosecreekite structure. With the conventional unweighted

* Contribution no. 404, from the Mineralogical Laboratory, Department of Geological Sciences, University of Michigan.

0003–004X/86/1112–1494$02.00

Table 2. Atomic coordinates ($\times 10^4$), anisotropic thermal coefficients ($\times 10^4$), and equivalent isotropic temperature factors ($B_{eq}$; Å$^2$)

| | $x$ | $y$ | $z$ | $\beta_{11}$ | $\beta_{22}$ | $\beta_{33}$ | $\beta_{12}$ | $\beta_{13}$ | $\beta_{23}$ | $B_{eq}$ |
|---|---|---|---|---|---|---|---|---|---|---|
| Ca | 6557(3) | 2721 | 1969(3) | 80(4) | 14(1) | 94(4) | −4(1) | 5(3) | 1(2) | 1.78 |
| Si(1) | 3374(3) | 4732(2) | 6282(3) | 69(5) | 7(1) | 72(5) | −4(2) | 34(4) | 1(2) | 1.18 |
| Si(2) | 3168(3) | 1294(2) | 5997(3) | 52(5) | 10(1) | 62(5) | −1(2) | 23(4) | −2(2) | 1.12 |
| SI(3) | 0219(3) | 2599(2) | 5249(3) | 57(5) | 6(1) | 62(5) | −1(2) | 18(4) | 2(2) | 1.03 |
| Si(4) | 1044(3) | 0578(2) | 8612(3) | 48(5) | 10(1) | 55(5) | −5(2) | 17(4) | −2(2) | 1.08 |
| Si(5) | 0892(3) | 3877(2) | 8325(3) | 61(5) | 9(1) | 51(5) | −2(2) | 23(4) | −2(2) | 1.07 |
| Si(6) | 2394(3) | 0045(2) | 2768(3) | 49(5) | 8(1) | 57(5) | −1(2) | 12(4) | 3(2) | 1.06 |
| Al(1) | 7482(3) | 1285(2) | 5887(4) | 45(5) | 8(1) | 59(5) | 1(2) | 13(4) | 4(2) | 1.00 |
| Al(2) | 0682(4) | 3982(2) | 2632(4) | 63(5) | 6(1) | 56(5) | 2(2) | 20(4) | 0(2) | 1.02 |
| O(1) | 7228(9) | 0612(4) | 4105(9) | 131(16) | 12(3) | 105(15) | −1(6) | 47(3) | 3(6) | 2.00 |
| O(2) | 5336(9) | 1478(4) | 6346(9) | 98(15) | 14(3) | 108(15) | 3(5) | 43(12) | −8(5) | 1.87 |
| O(3) | 8372(8) | 2097(4) | 5064(8) | 72(12) | 7(2) | 88(14) | −8(5) | 30(11) | 8(5) | 1.33 |
| O(4) | 9065(9) | 1001(4) | 7936(9) | 106(15) | 12(3) | 86(14) | −5(5) | 30(12) | 1(5) | 1.78 |
| O(5) | 2607(9) | 4392(4) | 8023(9) | 91(15) | 14(3) | 87(14) | −7(5) | 25(12) | 1(5) | 1.77 |
| O(6) | 2666(9) | 4226(4) | 4408(9) | 101(14) | 7(2) | 87(14) | 2(5) | 35(12) | 6(5) | 1.51 |
| O(7) | 5594(9) | 4662(4) | 7062(9) | 112(15) | 16(3) | 118(15) | −8(6) | 44(13) | −5(5) | 2.12 |
| O(8) | 2017(9) | 2065(4) | 5155(9) | 87(14) | 10(3) | 109(15) | 1(5) | 49(12) | 0(5) | 1.60 |
| O(9) | 2657(9) | 1069(4) | 7949(9) | 96(15) | 11(3) | 90(14) | −8(5) | 39(12) | −8(5) | 1.65 |
| O(10) | 2515(9) | 0596(4) | 4581(8) | 120(15) | 16(3) | 71(4) | −3(5) | 42(12) | 0(5) | 1.86 |
| O(11) | 0811(9) | 3051(4) | 7261(8) | 119(15) | 11(2) | 63(13) | −3(5) | 16(12) | −2(5) | 1.68 |
| O(12) | 9698(9) | 3179(4) | 3431(9) | 111(14) | 11(3) | 76(13) | 2(5) | 55(12) | 7(4) | 1.58 |
| O(13) | 9052(10) | 4718(4) | 2174(9) | 139(16) | 14(3) | 120(15) | 5(6) | 86(13) | 11(5) | 2.09 |
| O(14) | 1728(9) | 0585(4) | 0904(9) | 135(16) | 11(3) | 116(15) | −6(5) | 69(13) | −1(5) | 1.98 |
| O(15) | 1202(9) | 3741(4) | 0505(9) | 110(15) | 10(3) | 130(16) | −2(5) | 60(13) | 2(5) | 1.91 |
| O(16) | 9022(9) | 4346(4) | 7315(9) | 94(15) | 13(3) | 139(17) | 7(5) | 32(13) | 0(6) | 2.06 |
| $H_2O(1)$ | 3512(12) | 2234(6) | 0964(14) | 164(20) | 33(4) | 385(30) | −29(8) | 119(21) | −48(10) | 4.83 |
| $H_2O(2)$ | 6565(15) | 2989(6) | 8717(13) | 350(27) | 37(4) | 172(21) | 16(9) | 118(21) | 18(8) | 4.81 |
| $H_2O(3)$ | 5102(11) | 3063(5) | 4504(10) | 210(20) | 28(4) | 147(19) | 5(7) | 54(17) | 4(7) | 3.50 |
| $H_2O(4)$ | 7574(13) | 1530(5) | 1048(11) | 338(27) | 18(3) | 169(20) | 27(8) | 127(19) | 8(7) | 3.92 |
| $H_2O(5)$ | 5650(10) | 4074(5) | 1595(13) | 117(17) | 19(3) | 333(26) | −1(6) | 72(17) | 7(8) | 3.73 |

*Note:* E.s.d.'s are given in parentheses. The $y$ coordinate of Ca was held constant to fix the origin. Anisotropic temperature factors are of the form

$$\exp\left(-\sum_{i=1}^{3}\sum_{j=1}^{3} h_i h_j \beta_{ij}\right).$$

residual, $R$, at 0.32, a series of electron-density syntheses revealed the 21 nonequivalent oxygen atoms, inclusion of which in the structure factor calculations reduced the value of $R$ to 0.12. Dividing the tetrahedral cations into six Si and two Al atoms on the basis of cation–oxygen distances and the oxygens into sixteen framework and five water oxygens, the latter being those coordinated only to Ca, resulted in a decrease in $R$ to 0.075 after refining isotropic temperature factors. The correctness of this apportionment was confirmed by (1) the grand mean Si–O and Al–O distances of 1.61 and 1.73 Å, respectively, and (2) a calculation of empirical bond-valence sums (Brown, 1981) for all atoms excluding H.

Introduction of anisotropic temperature factors reduced the residual to its final values of 0.061 (unweighted) and 0.049 (weighted) for all 2017 reflections. Calculations of difference electron-density syntheses confirmed that all of the heavier atoms had been located but failed to disclose the positions of the hydrogens, a not unexpected result in view of the large isotropic temperature factors of the water oxygens (3.5 to 4.8 Å$^2$). The final results of the refinement are displayed in Tables 1 through 3, which list, respectively, the observed and calculated structure factors,[1] the positional and thermal parameters of the atoms including equivalent isotropic temperature factors (Hamilton, 1959), and selected interatomic distances and angles.

[1] To receive a copy of Table 1, order Document AM-86-323 from the Business Office, Mineralogical Society of America, 1625 I Street, N.W., Suite 414, Washington, D.C. 20006, U.S.A. Please remit $5.00 in advance for the microfiche.

## Discussion

The structure of goosecreekite (Fig. 1), like that of its Sr-Ba chemical analogue brewsterite, is based on distorted sheets of vertex-sharing tetrahedra layered parallel to (010) and centered at $y \approx 0$ and ½. Figure 2 shows a schematic diagram of one such layer, with the tetrahedral nodes linked by solid lines and the bridging oxygens omitted for clarity. The tetrahedral linkages define a network of edge-sharing 4-, 6-, and 8-membered rings, the ring systems of adjacent layers being roughly congruent. A view of the structure parallel to the layers (Fig. 3) exhibits a similar pattern. The same ring system also exists in each (010) tetrahedral layer of brewsterite, but there the rings are less distorted and adjacent layers are strictly congruent owing to mirror planes at $y = ¼$ and ¾. (The space group symmetry of brewsterite is $P2_1/m$ as opposed to $P2_1$ for goosecreekite.)

The essential difference between the two structures is the manner in which the layers are cross-linked in the **b** direction to form the 3-dimensional tectosilicate framework. In goosecreekite this linkage is accomplished through interlayer tetrahedra, $Si(3)O_4$, which are located approximately midway (at $y \approx ¼$ and ¾) between adjacent layers and which share two vertices with each layer (Fig. 3). In brewsterite the layers are cross-linked by interlayer oxygen

Table 3. Selected interatomic distances (Å) and angles (°)

| | | | | | | | |
|---|---|---|---|---|---|---|---|
| | | | $SiO_4$ and $AlO_4$ tetrahedra | | | | |
| Si(1)–O(6) | 1.593(7) | O(5)–Si(1)–O(7) | 103.5(3) | Si(5)–O(15) | 1.563(7) | O(5)–Si(5)–O(16) | 105.5(4) |
| Si(1)–O(7) | 1.594(7) | O(6)–Si(1)–O(7) | 109.6(4) | Si(5)–O(16) | 1.607(7) | O(11)–Si(5)–O(16) | 108.2(3) |
| Si(1)–O(1) | 1.601(7) | O(1)–Si(1)–O(5) | 110.2(4) | Si(5)–O(5) | 1.616(7) | O(5)–Si(5)–O(15) | 108.4(4) |
| Si(1)–O(5) | 1.634(7) | O(1)–Si(1)–O(7) | 110.4(4) | Si(5)–O(11) | 1.630(7) | O(11)–Si(5)–O(15) | 109.0(3) |
| Mean | 1.606 | O(5)–Si(1)–O(6) | 111.3(4) | Mean | 1.604 | O(5)–Si(5)–O(11) | 110.9(4) |
| | | O(1)–Si(1)–O(6) | 111.5(4) | | | O(15)–Si(5)–O(16) | 114.8(4) |
| | | Mean | 109.4 | | | Mean | 109.5 |
| Si(2)–O(10) | 1.585(7) | O(9)–Si(2)–O(10) | 106.6(3) | Si(6)–O(16) | 1.599(7) | O(7)–Si(6)–O(16) | 105.7(4) |
| Si(2)–O(2) | 1.589(7) | O(2)–Si(2)–O(8) | 107.4(4) | Si(6)–O(7) | 1.606(7) | O(10)–Si(6)–O(14) | 106.2(4) |
| Si(2)–O(9) | 1.616(7) | O(8)–Si(2)–O(9) | 108.2(3) | Si(6)–O(10) | 1.617(7) | O(7)–Si(6)–O(10) | 109.6(4) |
| Si(2)–O(8) | 1.622(7) | O(8)–Si(2)–O(10) | 110.5(4) | Si(6)–O(14) | 1.619(7) | O(14)–Si(6)–O(16) | 111.2(4) |
| Mean | 1.603 | O(2)–Si(2)–O(9) | 111.8(4) | Mean | 1.610 | O(7)–Si(6)–O(14) | 112.1(3) |
| | | O(2)–Si(2)–O(10) | 112.3(4) | | | O(10)–Si(6)–O(16) | 112.2(4) |
| | | Mean | 109.5 | | | Mean | 109.5 |
| Si(3)–O(3) | 1.598(6) | O(3)–Si(3)–O(12) | 105.0(4) | Al(1)–O(4) | 1.708(7) | O(1)–Al(1)–O(3) | 105.7(3) |
| Si(3)–O(11) | 1.621(6) | O(8)–Si(3)–O(11) | 106.7(4) | Al(1)–O(1) | 1.724(7) | O(3)–Al(1)–O(4) | 107.7(3) |
| Si(3)–O(12) | 1.630(7) | O(8)–Si(3)–O(12) | 109.7(3) | Al(1)–O(3) | 1.736(7) | O(2)–Al(1)–O(4) | 109.7(3) |
| Si(3)–O(8) | 1.640(7) | O(3)–Si(3)–O(11) | 111.2(3) | Al(1)–O(2) | 1.741(7) | O(1)–Al(1)–O(2) | 110.8(3) |
| Mean | 1.622 | O(3)–Si(3)–O(8) | 111.8(3) | Mean | 1.727 | O(2)–Al(1)–O(3) | 111.0(3) |
| | | O(11)–Si(3)–O(12) | 112.5(4) | | | O(1)–Al(1)–O(4) | 111.9(3) |
| | | Mean | 109.5 | | | Mean | 109.5 |
| Si(4)–O(4) | 1.596(7) | O(9)–Si(4)–O(14) | 104.4(3) | Al(2)–O(6) | 1.733(7) | O(6)–Al(2)–O(12) | 107.0(3) |
| Si(4)–O(13) | 1.599(7) | O(4)–Si(4)–O(14) | 109.0(4) | Al(2)–O(13) | 1.733(7) | O(12)–Al(2)–O(15) | 108.3(3) |
| Si(4)–O(14) | 1.612(7) | O(4)–Si(4)–O(9) | 110.3(4) | Al(2)–O(15) | 1.745(7) | O(13)–Al(2)–O(15) | 108.3(3) |
| Si(4)–O(9) | 1.643(7) | O(9)–Si(4)–O(13) | 110.5(4) | Al(2)–O(12) | 1.749(7) | O(12)–Al(2)–O(13) | 109.1(3) |
| Mean | 1.612 | O(13)–Si(4)–O(14) | 110.6(4) | Mean | 1.740 | O(6)–Al(2)–O(13) | 111.7(4) |
| | | O(4)–Si(4)–O(13) | 111.9(4) | | | O(6)–Al(2)–O(15) | 112.4(3) |
| | | Mean | 109.4 | | | Mean | 109.5 |

| $Ca(H_2O)_5O_2$-capped octahedron | | $(H_2O–H_2O)$ and $(H_2O–O) \leq 3$ Å | | | |
|---|---|---|---|---|---|
| Ca–$H_2O$(1) | 2.336(8) | $H_2O$(5)–O(13) | 2.69(1) | $H_2O$(3)–$H_2O$(1) | 2.92(1) |
| Ca–$H_2O$(4) | 2.367(8) | $H_2O$(3)–O(6) | 2.70(1) | $H_2O$(4)–O(4) | 2.93(1) |
| Ca–$H_2O$(2) | 2.419(9) | $H_2O$(4)–O(1) | 2.81(1) | $H_2O$(1)–O(9) | 2.94(1) |
| Ca–O(12) | 2.420(7) | $H_2O$(3)–$H_2O$(5) | 2.87(1) | $H_2O$(3)–$H_2O$(2) | 2.98(1) |
| Ca–$H_2O$(5) | 2.447(8) | $H_2O$(3)–O(3) | 2.89(1) | $H_2O$(4)–O(3) | 3.00(1) |
| Ca–$H_2O$(3) | 2.447(8) | | | | |
| Ca–O(3) | 2.544(6) | | | | |
| Mean | 2.426 | | | | |

*Note:* E.s.d.'s are given in parentheses. The $H_2O$(5) molecule caps the $Ca(H_2O)_5O_2$ octahedron.

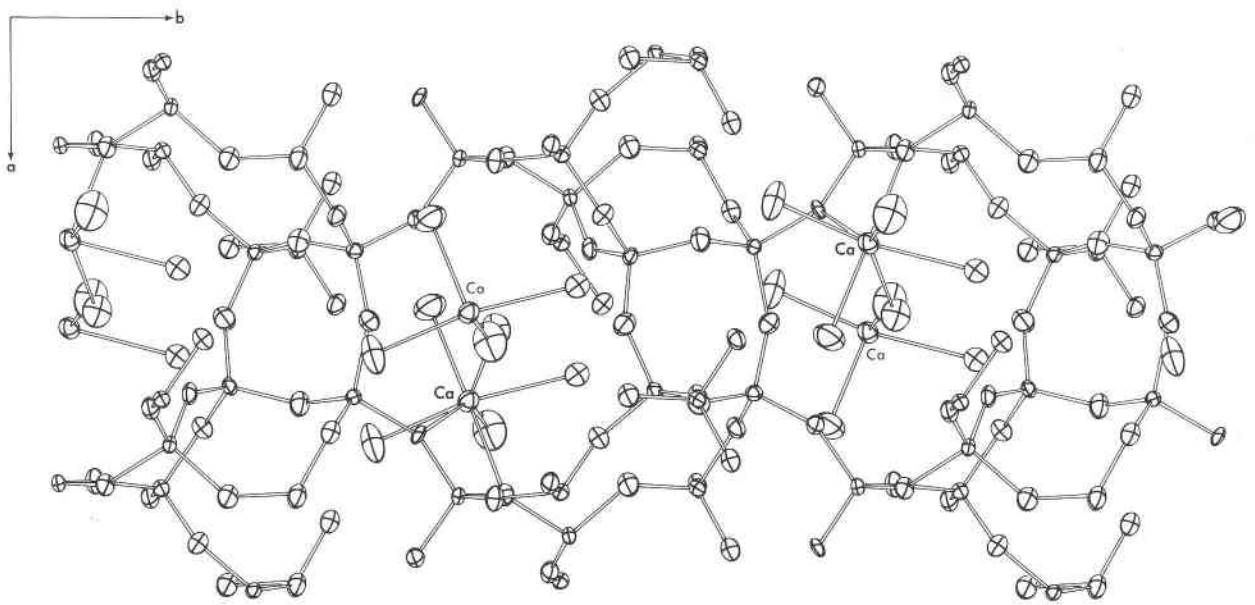


Fig. 1. The crystal structure of goosecreekite viewed down **c***, as drawn by ORTEP (Johnson, 1976). Ca atoms labeled in less-bold lettering lie in adjacent unit cells.

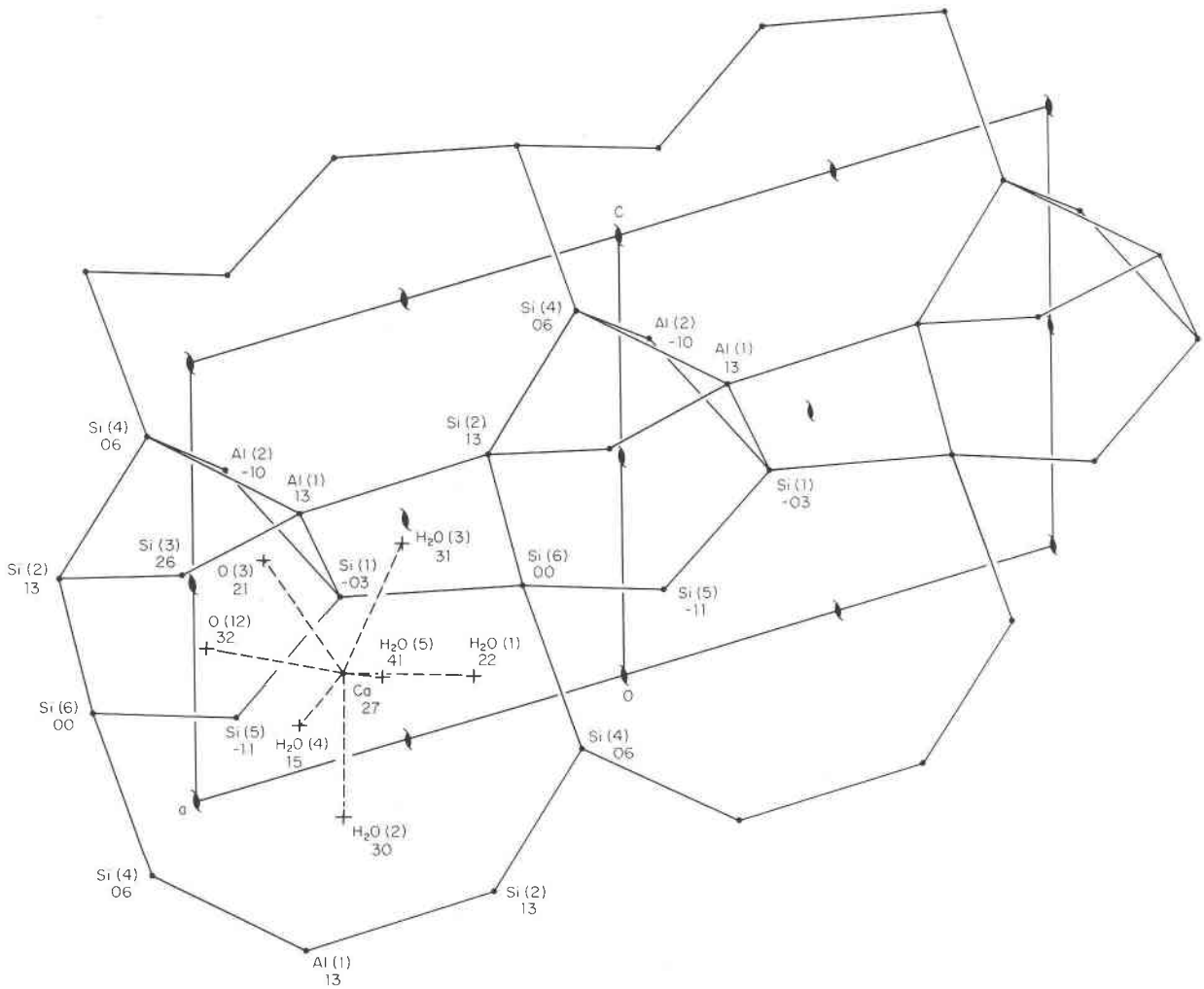


Fig. 2. Projection of the tetrahedral layer at $y \approx 0$ on (010), showing the linkage of tetrahedral cations into a network of 4-, 6-, and 8-membered rings. Bridging oxygens are omitted for clarity. The 8-rings define channels, which run through the structure in the **b** direction and contain the Ca atoms, one of which is shown with its O and $H_2O$ ligands. Numbers beneath the atom labels are atomic $y$ coordinates × 100.

atoms, O(9), located on the mirror planes at $y = \frac{1}{4}$ and $\frac{3}{4}$. Each such oxygen is shared by two tetrahedra, one from each of the two adjacent layers, in effect forming a $T_2O_7$ group, which Perrotta and Smith (1964) treated as the layer-linking structural element. In addition to differences in form, the cross-linking elements in goosecreekite ($TO_4$) and brewsterite ($T_2O_7$) differ in their location relative to the ring system of the tetrahedral layers. In the former mineral, each Si(3)$O_4$ group is approximately centered between two 6-rings of adjacent layers (Fig. 2), whereas in the latter, each $T_2O_7$ group is centered between the 8-rings. This difference has an important effect on the channel systems of the two minerals, a matter which will be considered presently.

In addition to its role as an interlayer cation, the Si(3) atom is notable in one other respect. The interatomic distances in Table 3 suggest that there is a small amount of Si-Al solid solution on the Si(3) and Al(1) sites. The mean bond distance of the former, 1.622 Å, is noticeably greater than those of the remaining Si sites, which range from 1.603 to 1.612 Å, and corresponds to a site occupancy of 88% Si and 12% Al using the empirical formula of Jones (1968). Similarly, the mean bond distance of the Al(1) site, 1.727 Å, corresponds to an occupancy of 79% Al and 21% Si. The relationship given by Smith (1974) yields somewhat lower values, namely 92% Si, 8% Al and 87% Al, 13% Si. In any case, it appears that there has, in effect, been an exchange of ca. 10 to 20% Si from Si(3) for a like amount of Al from Al(1) and vice versa. Since Si(3) and Al(1) share a common vertex (Fig. 2), this exchange avoids the violation of Loewenstein's rule that would occur if the only substitution were Al in the Si(3) site.

Such a redistribution of positive charge in the tetrahedral sites would be advantageous in two respects. First, the presence of a lower-valence substituent in Si(3) would

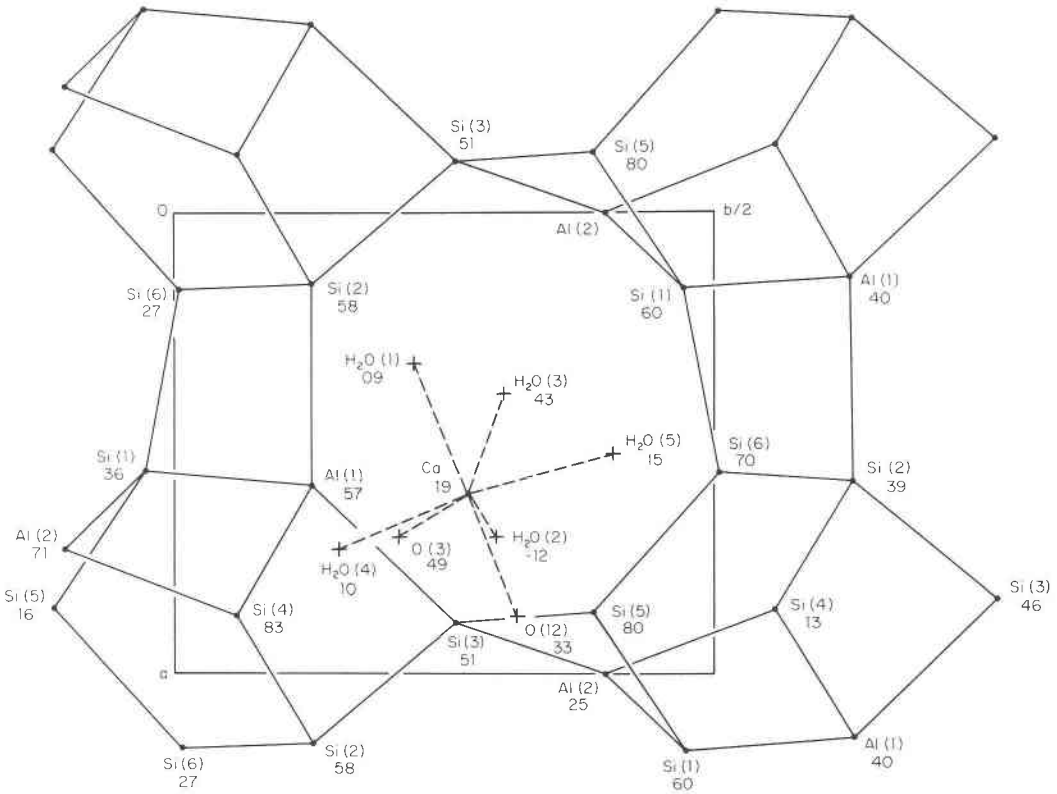


Fig. 3. Projection of the tetrahedral layers at $y \approx 0$ and ½ on (001), showing the linkage of layers through the Si(3) atom. The second set of structural channels, defined by 8-rings and running parallel to the **c*** direction, is also evident. Bridging oxygens are omitted. Numbers beneath the atom labels are the coordinates ($z \sin \beta$) × 100.

prevent overbonding of O(3) and O(12), which are both coordinated to Ca, Si(3), and one Al and which are the only oxygens bonded to more than two cations (Table 4). As things now stand, O(3) and O(12) have nearly ideal bond-valence sums, 2.03 and 1.98 v.u., respectively. Second, some Al in Si(3) should reduce cation–cation repulsion across the shared edge (defined by O(3)–O(12) = 2.562 Å in Figs. 2 and 3) of the $Si(3)O_4$ and $Ca(H_2O)_5O_2$ polyhedra. The distance Ca–Si(3) is a short 3.108 Å, which is comparable in magnitude to the shortest Si–Si distances

Table 4. Empirical bond-valence sums (v.u.) for the anions and cations

| | Ca | Si(1) | Si(2) | Si(3) | Si(4) | Si(5) | Si(6) | Al(1) | Al(2) | Σv |
|---|---|---|---|---|---|---|---|---|---|---|
| O(1) | | 1.06 | | | | | | 0.77 | | 1.83 |
| O(2) | | | 1.09 | | | | | 0.74 | | 1.83 |
| O(3) | 0.21 | | | 1.07 | | | | 0.75 | | 2.03 |
| O(4) | | | | | 1.07 | | | 0.80 | | 1.87 |
| O(5) | | 0.97 | | | | 1.02 | | | | 1.99 |
| O(6) | | 1.08 | | | | | | | 0.75 | 1.83 |
| O(7) | | 1.08 | | | | | 1.04 | | | 2.12 |
| O(8) | | | 1.00 | 0.95 | | | | | | 1.95 |
| O(9) | | | 1.02 | | 0.95 | | | | | 1.97 |
| O(10) | | | 1.10 | | | | 1.01 | | | 2.11 |
| O(11) | | | | 1.00 | | 0.98 | | | | 1.98 |
| O(12) | 0.28 | | | 0.98 | | | | | 0.72 | 1.98 |
| O(13) | | | | | 1.06 | | | | 0.75 | 1.81 |
| O(14) | | | | | 1.03 | | 1.01 | | | 2.04 |
| O(15) | | | | | | 1.17 | | | 0.73 | 1.90 |
| O(16) | | | | | | 1.04 | 1.06 | | | 2.10 |
| $H_2O(1)$ | 0.34 | | | | | | | | | 0.34 |
| $H_2O(2)$ | 0.28 | | | | | | | | | 0.28 |
| $H_2O(3)$ | 0.26 | | | | | | | | | 0.26 |
| $H_2O(4)$ | 0.31 | | | | | | | | | 0.31 |
| $H_2O(5)$ | 0.26 | | | | | | | | | 0.26 |
| Σv | 1.94 | 4.19 | 4.21 | 4.00 | 4.11 | 4.21 | 4.12 | 3.06 | 2.95 | |

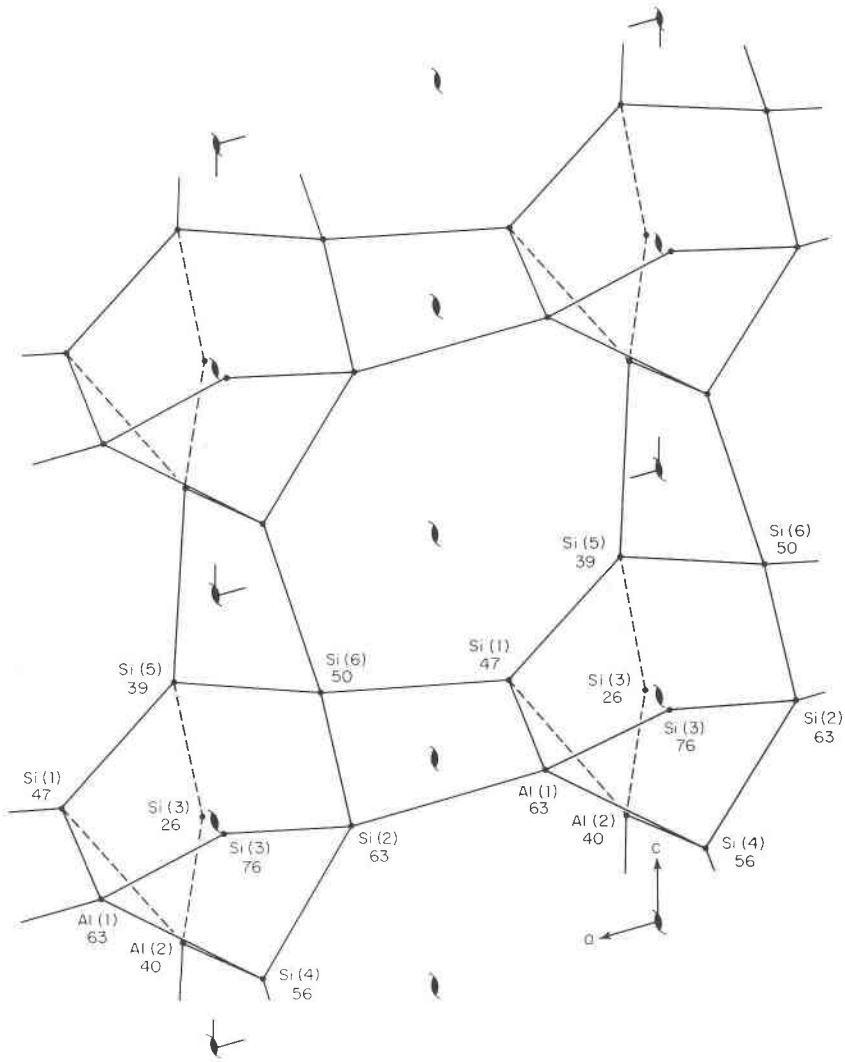


Fig. 4. Projection of the framework layer at $y \approx \frac{1}{2}$ on (010), showing the linkage of $T_9O_{18}$ units. Numbers beneath the atom labels are $y$ coordinates × 100.

in the tetrahedral framework. The next-nearest cation neighbors of the Ca atom are Al(2) at 3.688 Å and Al(1) at 3.724 Å.

Inferences about (Al,Si) disorder from the tetrahedral bond lengths cited above may be questioned, since the mean bond length for the Si(3) site differs by less than $3\sigma$ from those of the other Si sites, whereas that of the Al(1) site differs by only $2\sigma$ from that of Al(2). However, the presence of some Al in the Si site which shares an edge with the exchangeable cation polyhedron is supported by the occurrence of the same phenomenon in epistilbite (Perrotta, 1967), "disordered" epistilbite (Slaughter and Kane, 1969), brewsterite (Schlenker et al., 1977), and heulandite (Merkle and Slaughter, 1968; Alberti, 1972). In each of these structures the affected tetrahedral sites have three common characteristics: (1) They function as interlayer linkages; (2) they share an edge with the coordination polyhedron of the large cation (Ca, Na, Sr, or Ba); and (3) they have the highest degree of Al for Si substitution in the structure. This Ca-Al correlation does not exist in the structure of stilbite, however, as the latter atoms are almost completely disordered over the tetrahedral sites (Slaughter, 1970; Galli, 1971).

In the foregoing discussion the tetrahedral framework of goosecreekite has been described in terms of cross-linked layers, in part to emphasize its relationship to brewsterite. Alternatively, the framework can be described in terms of a periodic array of identical polyhedral units (Fig. 4), each unit being composed of a 6-ring from an (010) layer, two interlayer Si(3) atoms located above and below the plane of the 6-ring, respectively, and a 4-ring defined by Si(1), Si(4), Al(1), and Al(2). The resulting polyhedron is composed of two 6-rings and three 4-rings and has the composition $(Si_7Al_2)O_{18}$ or $T_9O_{18}$. Each such unit shares two vertices [the Si(3) atoms at $y = 0.26$ and 0.76] to form chains in the **b** direction. Adjacent

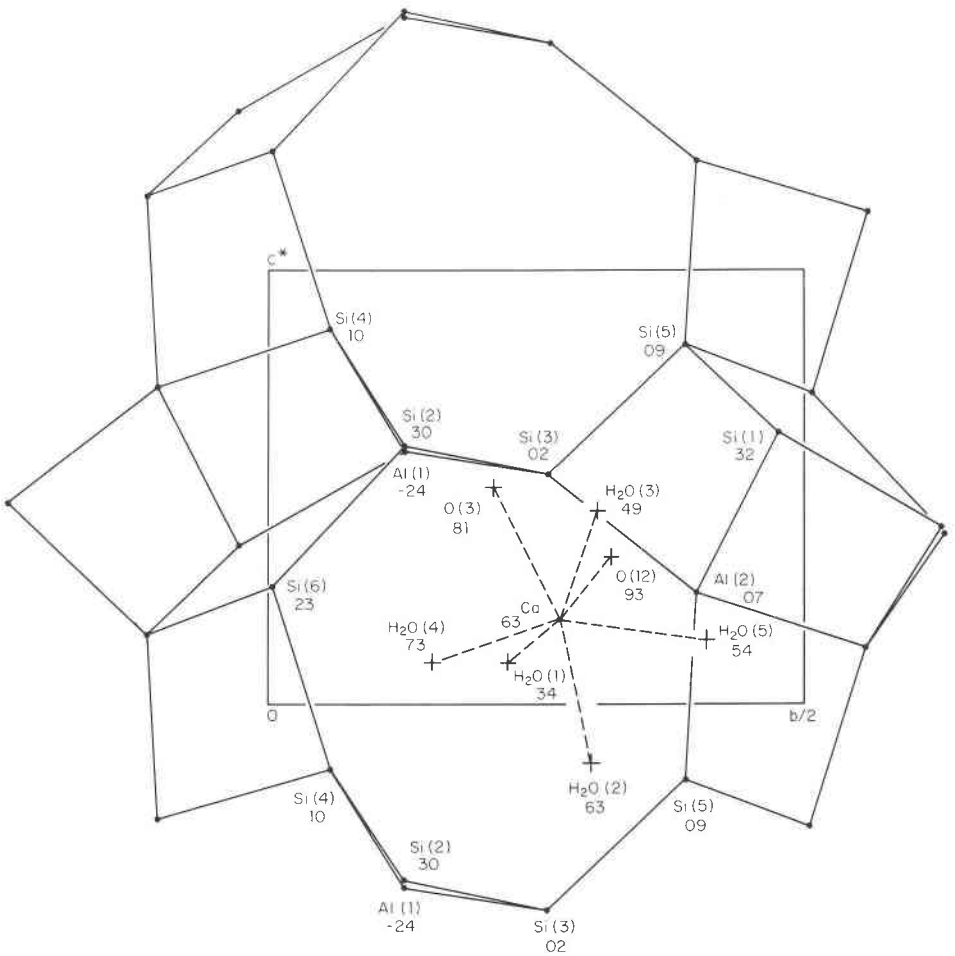


Fig. 5. Projection of the tetrahedral layers at $y \approx 0$ and ½ on (100)*, showing the third set of channels in goosecreekite, this one running parallel to the **a** direction and defined by 8-rings. Bridging oxygens are omitted. Numbers beneath the atom labels are the coordinates ($x \sin \beta$) × 100.

chains are then cross-linked by additional 4-rings in the **a** and **c** directions to form a 3-dimensional network.

The periodic array of $T_9O_{18}$ units constitutes the entire tetrahedral framework of goosecreekite, a fact which would seem to qualify that group as the secondary building unit (SBU) of the structure. In fact, $T_9O_{18}$ fits neatly between the $T_8O_{16}$ SBU, which is characteristic of the mordenite group, and the $T_{10}O_{20}$ SBU of the heulandite group. However, it is not one of the eight SBUs originally defined by Meier (1968), nor does it appear among the nine SBUs in the more recent tabulation of Gramlich-Meier and Meier (1982). Since these SBUs are the basis for the division of the zeolites into groups in the currently accepted structural classification, there is some question as to where goosecreekite belongs in this scheme. Despite its obvious chemical and structural affinities to brewsterite, it cannot be placed in the heulandite group because it lacks the $T_{10}O_{20}$ or "4-4-1" SBU which defines that group. The fact that the apparent SBU of goosecreekite is composed 4- and 6-rings and every tetrahedral atom is a member of a single 4-ring would seem to place it in the analcime group (Meier, 1968). However, this assignment seems artificial since, unlike goosecreekite and the heulandite group, analcime and its congeners are not layer structures. The position of goosecreekite in the zeolite classification scheme therefore remains somewhat ambiguous.

The goosecreekite structure contains three sets of channels, each bounded by 8-rings and running parallel, respectively, to the **a, b,** and **c*** axes of the unit cell. The channels parallel to **b** differ from the other sets in that they follow a zig-zag course through the structure. This is because the 8-rings that define them are highly asymmetrical (Fig. 2), and successive rings normal to **b** are rotated 180° by the screw axis at (½,*y*,0). Each of Figures 2, 3, and 5 shows one of the channel types in cross-section, as well as one of the Ca ions resident within the channels. These ions, with their attendant water molecules, are located approximately at the intersections of the three channel systems, but adjacent to the channel walls rather than at their centers. Each Ca is bonded to two framework oxygens, O(3) and O(12), and to all five water molecules. The coordination polyhedron thus defined is a highly dis-

torted monocapped octahedron, with $H_2O(5)$ being the capping ligand.

Comparing the channel network and exchangeable cation coordination in goosecreekite with those of brewsterite, the latter mineral also has channels bounded by 8-rings and oriented parallel to **a** and **c***. There are, however, no channels in the **b** direction. This happens because, as previously noted, the linkage of (010) layers in brewsterite occurs through the 8-rings; the analogous 8-rings in goosecreekite are clear of obstructing tetrahedra, owing to the fact that interlayer connections are through the 6-rings. Being larger than $Ca^{2+}$, the $Sr^{2+}$ and $Ba^{2+}$ ions have higher coordination numbers, bonding to five water molecules and four framework oxygens (as opposed to only two in goosecreekite). The latter fact suggests that the large cations in goosecreekite might be more easily exchangeable than those in brewsterite, but this may be negated by the increased strength of the Ca–O bond relative to Ba–O and Sr–O. On the other hand, the presence of an additional set of channels in goosecreekite should make it more amenable to ionic and molecular diffusion.

Since the H atoms could not be located experimentally, nothing can be said with certainty about H bonding by the water molecules in goosecreekite. However, comparison of those $H_2O$–O distances less than 3.0 Å (the sum of the van der Waals radii of oxygen) in Table 3 with the bond-valence sums in Table 4 reveals some suggestive correlations. Three of the four framework oxygens having bond valence sums less than 1.9 v.u. [O(1), O(6), and O(13)] are involved in the three shortest $H_2O$–O approaches in the structure. These distances, $H_2O(5)$–O(13) 2.69 Å, $H_2O(3)$–O(6) 2.70 Å, and $H_2O(4)$–O(1) 2.81 Å, all fall within the range of the majority of known O–H . . . O bonds lengths (2.6 to 2.8 Å). The fourth underbonded oxygen, O(2), is a more distant 3.06 Å from the nearest water molecule, $H_2O(3)$, but even this distance is within the upper limit for a H bond. By comparison, a study of the H-bonding system in brewsterite using neutron diffraction to locate the protons (Artioli et al., 1985) found O–H . . . O distances in the range 2.887 to 3.287 Å, all of which are longer than the proposed H-bond distances in goosecreekite, discounting $H_2O(3)$–O(2). It seems likely, therefore, that a system of H bonds exists in goosecreekite and that the goosecreekite system of H bonds is stronger than that in brewsterite.

## References


Alberti, Alberto. (1972) On the crystal structure of the zeolite heulandite. Tschermaks Mineralogische und Petrographische Mitteilungen, 18, 129–146.

Artioli, Gilberto, Smith, J.V., and Kvick, Åke. (1985) Multiple hydrogen positions in the zeolite brewsterite, $(Sr_{0.95}Ba_{0.05})Al_2Si_6O_{16}\cdot 5H_2O$. Acta Crystallographica, C41, 492–497.

Barrer, R.M. (1984) Zeolite structures. In F. Ramôa Ribeiro et al., Eds. Proceedings of the NATO Advanced Study Institute on Zeolites: Science and Technology, 35–81.

Brown, I.D. (1981) The bond-valence method: An empirical approach to chemical structure and bonding. Structure and Bonding in Crystals, 2, 1–30.

Doyle, P.A., and Turner, P.S. (1968) Relativistic Hartree-Fock X-ray and electron scattering factors. Acta Crystallographica, A24, 390–397.

Dunn, P.J., Peacor, D.R., Newberry, Nancy, and Ramik, R.A. (1980) Goosecreekite, a new calcium aluminum silicate hydrate possibly related to brewsterite and epistilbite. Canadian Mineralogist, 18, 323–327.

Finger, L.W. (1972) RFINE 2: A Fortran IV computer program for structure factor calculation and least-squares refinement of crystal structures. Geophysical Laboratory, Washington, D.C.

Frondel, Clifford, and Hurlbut, C.S., Jr. (1955) Determination of the atomic weight of silicon by physical measurements on quartz. Journal of Chemical Physics, 23, 1215–1219.

Galli, Ermanno. (1971) Refinement of the crystal structure of stilbite. Acta Crystallographica, B27, 833–841.

Gramlich-Meier, Rachel, and Meier, W.M. (1982) Constituent units and framework conformations in zeolite networks. Journal of Solid State Chemistry, 44, 41–49.

Hamilton, W.C. (1959) On the isotropic temperature factor equivalent to a given anisotropic temperature factor. Acta Crystallographica, 12, 609–610.

Johnson, C.K. (1976) ORTEP-II: A Fortran thermal-ellipsoid plot program for crystal structure illustrations. Report ORNL-5138, Oak Ridge National Laboratory, Oak Ridge, Tennessee.

Jones, J.B. (1968) Al–O and Si–O tetrahedral distances in aluminosilicate framework structures. Acta Crystallographica, B24, 355–358.

Main, Peter. (1978) MULTAN 78: A system of computer programmes for the automatic solution of crystal structures from X-ray diffraction data. University of York, York, England.

Meier, W.M. (1968) Zeolite structures. In Molecular sieves, 10–27. Society of Chemical Industry, London.

Merkle, A.B., and Slaughter, Maynard. (1968) Determination and refinement of the structure of heulandite. American Mineralogist, 53, 1120–1138.

Perrotta, A.J. (1967) The crystal structure of epistilbite. Mineralogical Magazine, 36, 480–490.

Perrotta, A.J., and Smith, J.V. (1964) The crystal structure of brewsterite, $(Sr,Ba,Ca)(Al_2Si_6O_{16})\cdot 5H_2O$. Acta Crystallographica, 17, 857–862.

Schlenker, J.L., Pluth, J.J., and Smith, J.V. (1977) Refinement of the crystal structure of brewsterite, $Ba_{0.5}Sr_{1.5}Al_4Si_{12}O_{32}\cdot 10H_2O$. Acta Crystallographica, B33, 2907–2910.

Slaughter, Maynard. (1970) Crystal structure of stilbite. American Mineralogist, 55, 387–397.

Slaughter, Maynard, and Kane, W.T. (1969) The crystal structure of a disordered epistilbite. Zeitschrift für Kristallographie, 130, 68–87.

Smith, J.V. (1974) Feldspar minerals. I. Crystal structure and physical properties, 70. Springer-Verlag, Heidelberg.



Manuscript received June 24, 1985
Manuscript accepted July 8, 1986